N90-18984

ANNIHILATION PHYSICS OF EXOTIC GALACTIC DARK MATTER PARTICLES

F. W. Stecker
Laboratory for High Energy Astrophysics
NASA Goddard Space Flight Center
Greenbelt, MD 20771, U.S.A.

ABSTRACT

Various theoretical arguments make exotic heavy neutral weakly interacting fermions, particlularly those predicted by supersymmetry theory, attractive candidates for making up the large amount of unseen gravitating mass in galactic halos. Such particles can annihilate with each other, producing secondary particles of cosmic-ray energies, among which are antiprotons, positrons, neutrinos and γ-rays. Spectra and fluxes of these annihilation products can be calculated, partly by making use of e^+e^- collider data and QCD models of particle production derived therefrom. These spectra may provide detectable signatures of exotic particle remnants of the big bang.

INTRODUCTION

Astronomers have learned that there is much more to the universe than meets the eye[1]. The discovery that the rotation curves of spiral galaxies are quite flat to radii as far out as can be observed indicates the presence of dark matter comprising most of the mass in galactic halos and which could also dominate the mass of the universe[2]. This dark matter is most likely of non-baryonic form[3]. It may be made up of exotic new particles, perhaps such as those predicted by supersymmetry theory[4]. The large body of literature on various aspects of the dark matter problem and dark matter detection[5] have recently been reviewed.

Possible candidates for dark matter are exotic, stable, weakly interacting particles, which we hereafter call χ particles. Among these, the "neutralinos" predicted by supersymmetry theory should be left over as relics of the early big-bang in cosmologically significant densities[6,7]. Such particles can annihilate to produce baryons of cosmic-ray energies as well as other familiar particles whose decays will produce cosmic-ray leptons (electrons, positrons and neutrinos) and also cosmic γ-rays. The fluxes and energy spectra of these "ordinary particles" resulting from the annihilation of various χ particles can be calculated. The annihilation process will produce a characteristic high energy cutoff in these spectra at the rest mass energy of the χ particle, typically ~5 to ~30 GeV. The Lund Monte Carlo[8] simulation technique used by particle physicists in comparing with e^+e^- collider data provides a powerful tool for predicting $\chi\chi$ annihilation spectra[9-13], since the process of quark-antiquark pair production is involved in both cases. We will present and discuss detailed energy spectra from the annihilation of χ particles in the Galaxy and show how the features of these spectra may help lead to indirect evidence of exotic dark matter particles.

The lightest of the neutral supersymmetric particles, designated the LSP, would be stable by virtue of a new natural conservation law called R-parity conservation, since it is the lightest state with odd R-parity. The mass eigenstate "neutralino" can be a pure state, but is more generally a superposition of the "higgsino" ($\tilde{h}$), "photino" ($\tilde{\gamma}$) and "zino", which are mixed by gauge and supersymmetry breaking. There is also the possibility that the χ particle could be a heavy Dirac neutrino. However, unlike the case with the LSP, there is no natural way of forbidding the decay of a "conventional" heavy neutrino. There is also experimental evidence

against dark matter heavy Dirac neutrinos.[14]

DARK MATTER ANNIHILATION

The basic physical processes involved in the $\chi\chi$ annihilation process are portrayed schematically in Fig 1. In the first stage of the annihilation (Stage "a" in Fig. 1), χ particles annihilate via a propagator Δ (e.g., a scalar fermion in the case of photinos and a Z particle in the case of higgsinos). These supersymmetric neutralinos are Majorana fermions, i.e., they are self annihilating. Then, (b) the annihilation usually produces a quark antiquark pair ($\chi\chi \rightarrow q\bar{q}$). This is followed by (c) a cascade of the quarks down to the mass shell by successive gluon emission, producing a quark-gluon shower and (d) conversion of the shower gluons into other quark antiquark pairs which (e) produce hadrons, followed by (f) the decay of the unstable hadrons. The hadronic showers carry the momentum of the original quark pair and so come out as two collimated "jets". Sometimes a hard gluon is also emitted in the process $\chi\chi \rightarrow q\bar{q}g$, which results in three jets. (More rarely two or more gluons can be produced.) The quark cascading and fragmentation processes must be described by quantum chromodynamics (QCD) models. The Lund simulation is based on a string fragmentation model of QCD interactions, with parameters determined from the e^+e^- collider data. However, it enables one to take account of the different fragmentation effects associated with various quark species. It thus provides a framework for extrapolating from e^+e^- collider data to determine $\chi\chi$ annihilation spectra from differing mixtures of final state quark jets.

Simulation of a $\chi\chi$ annihilation begins by selecting a fermion-antifermion final state according to the branching ratios (B.R.) appropriate for a given type of χ particle which depend on the mass (m_f) and charge (Q_f) of the fermion (quark or lepton) involved (B.R. ~ $\beta_f m_f^2 Q_f^4$ for photino ($\tilde{\gamma}$) annihilation; B.R. ~ $\beta_f m_f^2$ for higgsino and Majorana neutrino (ν_M) annihilations (Ref. 15, hereafter called RS).

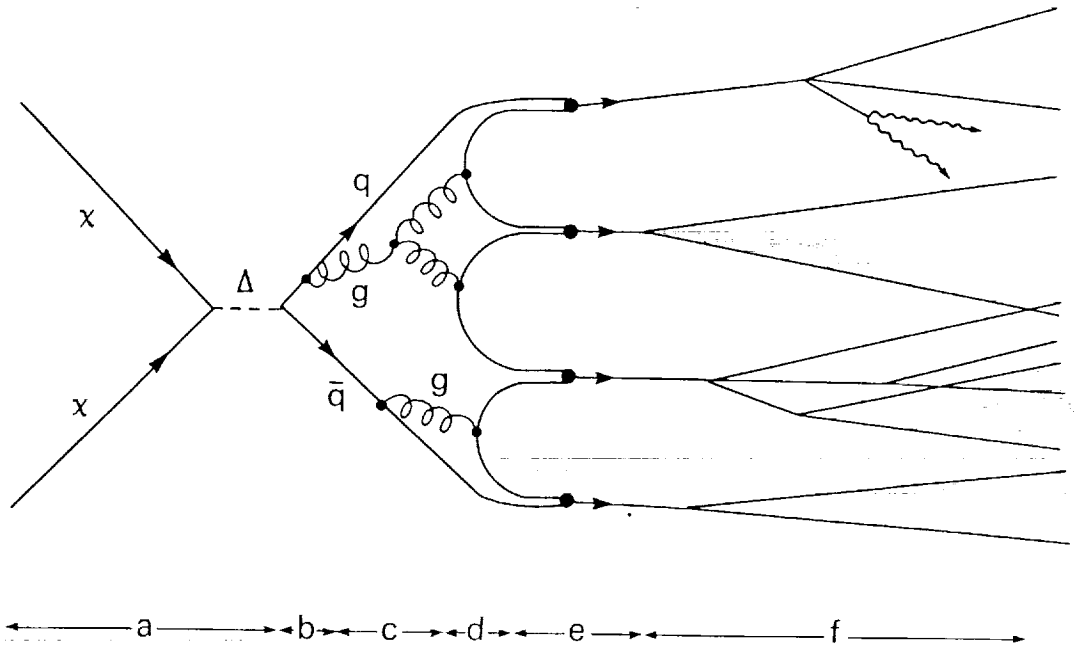

Fig. 1. Schematic diagram of the physics of χ particle annihilation with the various stages of the secondary particle production described in the text.

ANTIPROTON PRODUCTION

The energy spectrum of cosmic-ray antiprotons from photino annihilation was first calculated by Stecker, Rudaz and Walsh[16] (SRW), using $\bar{p}$ data obtained in e^+e^- collider experiments. They deduced from their results the fascinating possibility of explaining the entire observed spectrum of cosmic-ray $\bar{p}$'s as arising from the annihilation of 15 GeV χ particles. RS extended the spectral calculations to antiprotons, γ-rays and positrons, considering photinos, higgsinos and Majorana neutrinos as dark matter. Using the basic approach and formalism first given by SRW and RS, Stecker and Tylka[11] (ST1) extended the study of the antiproton spectrum with Lund Monte Carlo simulations, also taking account of recent upper limits on the low energy (< 0.5 GeV) cosmic-ray antiproton flux[17,18].

SRW and RS argued that the spectra of antiprotons and γ-rays would be quite similar to those observed for these products in e^+e^- collider experiments, owing to the universality of quark jet hadronization. However, e^+e^- annihilations produce a different mixture of heavy and light quark jets than that from $\chi\chi$ annihilations (e.g., higgsino annihilation produces final states with a very rich mixture of b quark jets). Collider data show that b and c quark jets carry off only 80% and 60% of the cms energy respectively. Thus, the results presented by SRW and RS should be considered to be a strict upper limit to the hardness of the $\chi\chi$ annihilation spectra.

As expected, the Lund simulation gives a significantly softer spectrum for final states weighted by heavy quark channels than that observed in e^+e^- experiments. Fig. 2 shows the inclusive antiproton production function in terms of the scaling variable $x = E/M_\chi$ for higgsinos (and Majorana neutrinos) or photinos of mass M_χ obtained from the Lund simulation.[11] E and β are the total $\bar{p}$ energy and velocity respectively. It should be noted that the cases of generic higgsinos and Majorana neutrinos of equal mass give identical results, as discussed by RS. Note that for χ annihilations at rest the cms energy is $2M_\chi$.

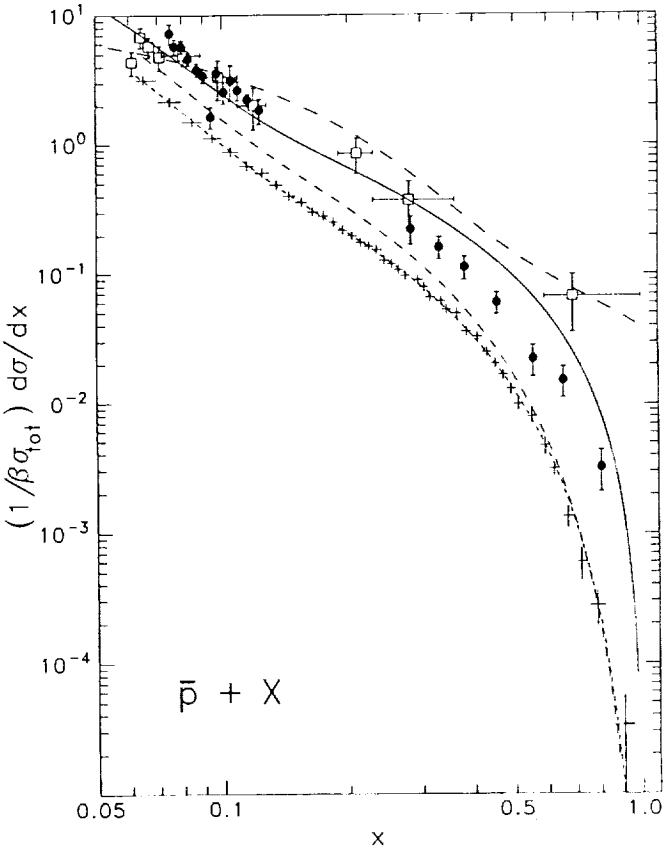

Fig. 2. Antiproton production spectra. Collider data are shown and compared with Lund prediction for e^+e^- annihilation (solid curve). Lund predictions for 15 GeV $\bar{h}\bar{h}$ (middle dashed curve) and $\tilde{\gamma}\tilde{\gamma}$ (lower dashed curve) annihilation are also shown. The crosses show the Lund data points.

The χ annihilation spectra are compared with the spectral function obtained from the Lund simulation of e^+e^- annihilations at a collider cms energy of 35 GeV (ST1). The e^+e^- collider data are also shown. Fig. 2 also shows the spectral source function used by RS to fit the TASSO data (upper dashed curve). The e^+e^- data do not include the antiprotons from $\bar{n}$ decay, however $\bar{n}$ decay was included in the $\chi\chi$ annihilation calculations. For comparison with the e^+e^- and $\chi\chi$ annihilation spectra in Fig. 2, the $\chi\chi$ spectra were

multiplied by a factor of 0.5. ST1 fit the results from the Lund Monte Carlo runs to simple analytic functions of the form

$$\zeta_{\bar{p}} f(x)/\beta \equiv (1/\beta\sigma)(d\sigma/dx) = A \exp(-\alpha x) + B(1-x)^{\delta}/x \qquad (1)$$

where $\zeta_{\bar{p}}$ is the number of $\bar{p}$'s per annihilation and f(x) normalized so that its integral is 1. This functional form reproduces the exponential dependence of the spectrum on x for low values of x. The second term dominates for $x > 0.15$ and goes smoothly to 0 at $x = 1$. The following source function fits to the parameter sets (A,α,B,δ) in eq. (1) were found: (a) For the e^+e^- collider simulation, (82, 46, 0.21, 2.13), (b) for 15 GeV higgsinos or Majorana neutrinos, (148, 50, 0.34, 4.39), and for 15 GeV photinos, (101, 50, 0.20, 3.99).

Photinos produce only ~2/3 as many antiprotons as generic higgsinos or Majorana neutrinos (0.2 per annihilation as opposed to 0.3). Much of this difference is due to the τ production channel, which is unimportant in higgsino annihilation but which accounts for 56% of photino annihilations and produces no baryons. (It should be noted that baryon-antibaryon production through quark jets is not as well understood as meson production (see discussion in ST1 and references therein.))

The production rate of antiprotons from $\chi\chi$ annihilation in the halo is

$$Q_{\bar{p}}(E) = n_{\chi}^2 \langle\sigma_{\chi} v\rangle_A f_{\bar{p}}(E) \qquad (2)$$

where $f_{\bar{p}}(E) = dN_{\bar{p}}/dE$, normalized to the number of antiprotons per annihilation. For example, in the case of $\tilde{h}$'s, the annihilation cross-section $\langle\sigma v\rangle_A$ is overwhelmingly dominated by the contributions of τ leptons and c and b quarks in the final state and is

$$\langle\sigma_{\chi} v\rangle_A = \frac{G_F^2}{4\pi}\left(m_{\tau}^2 + 3m_c^2 + 3m_b^2 \right) = 1.3 \times 10^{-26} \ \mathrm{cm}^3\mathrm{s}^{-1}. \qquad (3)$$

The antiprotons come from the hadronic $c\bar{c}$ and $b\bar{b}$ final states, but these account for a fraction $\delta_h \simeq 30/31 \simeq 1$ of the total. The ratio of $\bar{p}$ yields from photino and generic higgsino annihilation is

$$Q_{\bar{p}}^{\tilde{\gamma}} / Q_{\bar{p}}^{\tilde{h}} = \left[\delta_h^{\tilde{\gamma}} \langle\sigma_{\tilde{\gamma}} v\rangle_A / \delta_h^{\tilde{h}} \langle\sigma_{\tilde{h}} v\rangle_A\right] \simeq 9.4 \times 10^{-2} (m_W/m_{\tilde{q}})^4 \leq 0.1 \qquad (4)$$

where $m_W \simeq 81$ GeV is the W boson mass and $m_{\tilde{q}}$ is the mass of the squark (scalar quark) that mediates the $\tilde{\gamma}$ annihilation (RS).

The interstellar antiproton spectrum is of the form (from eq.(1))

$$I(E) = (4\pi)^{-1} (\rho_{\chi}^2/M_{\chi}^3) \langle\sigma_A v\rangle_{\chi} c\tau\beta^2 \{A\exp[-\alpha E/M_{\chi}] + BM_{\chi}[1-(E/M_{\chi})]^{\gamma}/E\} \qquad (5)$$

where ρ_{χ} is the mass density of dark matter and τ is the effective residence time of cosmic-ray antiprotons in the Galaxy. As pointed out by SRW and RS, eq. (5) for the interstellar spectrum must be modulated to take account of the effects of the solar wind on the spectrum observed at Earth. To do this, ST1 used a numerical integration of the spherically symmetric solution of the Fokker-Planck equation.

Fig. 3 shows the resultant $\bar{p}/p$ ratio as a function of energy for higgsino and photino annihilation as compared with the present antiproton data, the calculated spectrum of antiprotons from cosmic-ray collisions and the possible spectrum of extragalactic primary antiprotons in the baryon symmetric cosmology, also modulated[11] (ST1). For the higgsino case, the results are shown for both solar

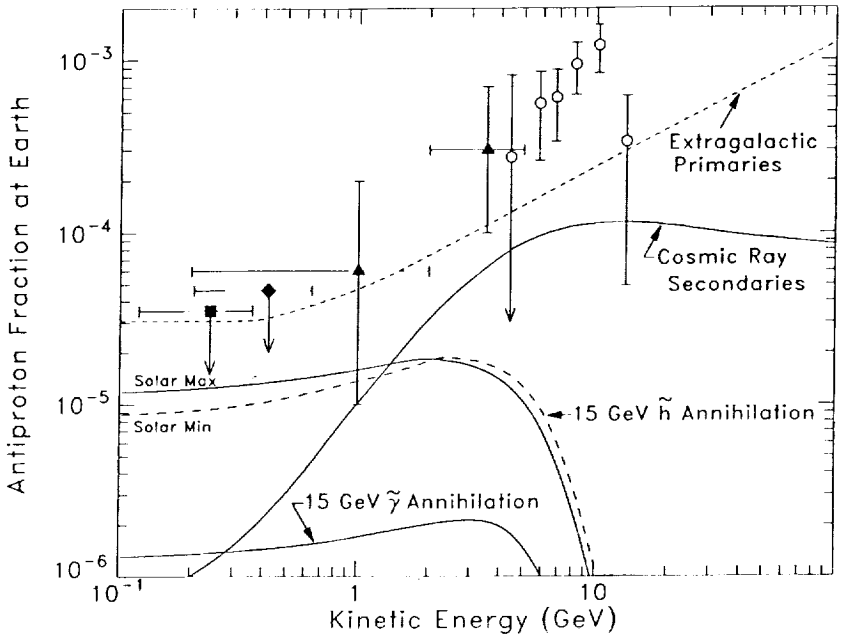

Fig. 3. The ratio $\bar{p}/p$ as a function of kinetic energy given for the different theoretical models (ST1). The data are as follows: (Ref. 17) - black square; (Ref. 18) - black diamond; (Ref. 19) - black triangles; (Ref. 20).

maximum and solar minimum. The annihilation spectra are shown for $\tau = 10^8$ y and $\rho_\chi = 0.3$ GeV cm^{-3}. For generic higgsinos, $\langle\sigma_A v\rangle = 1.26 \times 10^{-26}$ cm^{3}s^{-1}. In the photino case, ST took a minimal squark mass of 80 GeV, giving $\langle\sigma v\rangle = 0.22 \times 10^{-26}$ cm^{3}s^{-1}. It is clear from the figure that fluxes which are consistent with the upper limits[18,19] on the low energy antiprotons cannot account for the reported fluxes of antiprotons in the energy range around 10 GeV.

These results can be used to test for constraints on χ particles. The residence time τ is $\sim 10^8$ y for halo propagation[21] and $\sim 2\times10^7$ y for disk propagation models[22]. Studies of cosmic-ray electrons and secondary nuclei[23,24] appear to indicate that τ cannot be too much less than 2×10^7 y or too much more than 10^8 y. The density ρ_χ is probably in the range $\sim$0.2 to $\sim$0.4 GeV cm^{-3}.[25] The generic higgsino value for the cross section from eq. (3) is probably an upper limit to what one would expect for a χ annihilation cross section and significant values for the χ masses lie in the range of $\sim$5 to $\sim$30 GeV (RS). For photinos the cross sections can be much smaller than for higgsinos (see eq. (4)). Thus, $r_5 \equiv 10^5\,(\bar{p}/p)_{24}$ is at most $\sim$10 (for 15 generic GeV higgsinos) but can easily be as low as $\sim 4\times10^4 \langle\sigma v\rangle \ll 1$. The experimental upper limit $r_5 \leq 3.5$ is consistent with an acceptable range of astrophysical parameters for all χ particles of interest. The relevant supersymmetric parameters can be adjusted to give cosmological densities of interest for values of M_χ between $\sim$5 and $\sim$30 GeV. Generic higgsinos or Majorana neutrinos with $M_\chi = 15$ GeV will give $\Omega_\chi h_{50}^2 = 0.2$. It is possible to generalize the values for the vacuum expectation values of the Higgs fields (see eq. (3) of RS) if one wishes to obtain $\Omega_\chi h_{50}^2 = 1$ (the inflation cosmology prediction) with 15 GeV higgsinos. Note that one requires $\Omega_\chi h_{50}^2$ of at least $\sim$0.1 to obtain dark matter halos. (As usual, Ω is the fraction of the critical density in χ particles and h_{50} is the Hubble constant in units of 50 km s^{-1} Mpc^{-1}.)

The present upper limits on low energy $\bar{p}$'s do not constrain dark matter models. However, with the possible range of values for r_5 given above, it is possible to hunt for evidence of χ's with low energy $\bar{p}$ experiments, perhaps at a level not too far below the present limits. Upper limits on the order of $r_5 \leq 0.1$ would place significant constraints on dark matter models.

THE COSMIC-RAY NEUTRINO SPECTRUM FROM $\chi\chi$ ANNIHILATION

There are four main sources of neutrinos and positrons from $\chi\chi$ annihilation to consider, viz., first generation prompt leptons, second generation prompt leptons and charged π and K meson decay leptons (RS). Charmed and bottom quarks and τ leptons are efficient sources of prompt, high energy leptons and antileptons from their weak decays. E.g., for neutrino-positron production, the relevant decay chains are as follows (W^* is a virtual W boson):

$$\tau^+ \to \bar{\nu}_\tau + W^{+*}$$
$$\bar{b} \to \bar{c} + W^{+*} \qquad (6)$$
$$\text{and} \quad c \to s + W^{+*}$$

with W^{+*} decaying to $\ell^+\nu_\ell$, where $\ell^+ = e^+$ or μ^+ (for b decays, $\ell = \tau$ is considerably suppressed by phase space and will be neglected here). B.R.'s for these decays are 18% for τ and 13% for both b and c. Leptons also come from second generation prompt processes given by the decay chains $\tau\to\mu\to e$, $c\to\mu\to e$, $b\to\mu\to e$ and $b\to c\to e$. The B.R. for the first chain is 18%; that of the last three is 13%.

The neutrino flux from the decay of π mesons produced in heavy fermion annihilations can be determined by using the e^+e^- collider data. Within experimental error, the data for the pion production spectrum from e^+e^- annihilations with cms energies above 14 GeV can be fitted to a single spectral function having the form (RS).

$$\zeta_\pi f(E_\pi) = \beta_\pi (11.6\, e^{-1.13E_\pi} + 1.35\, e^{-0.46E_\pi}) \quad \text{GeV}^{-1}. \qquad (7)$$

where, $\beta = [1-(m_\pi/M_\chi)^2 x^{-2}]^{1/2}$, ζ_π is the pion multiplicity per annihilation. The low energy pion-decay neutrinos, which peak at ~35 MeV, can be calculated using the well-known kinematical formulae. At energies >> 35 MeV, the π-decay neutrino spectrum may be approximated by noting that two pairs of ν_μ, $\bar{\nu}_\mu$ and one pair of ν_e, $\bar{\nu}_e$ are produced for each e^+, e^- pair produced in the annihilations. All of these leptons take about 1/4 each of the pion energy. It follows from eq. (7) that

$$I_{(\pi)}(E) = \frac{Q_{(\pi)}(E)c\tau}{4\pi} = \frac{n_\chi^2 \langle\sigma_\chi v\rangle_A c\tau}{4\pi} (5.4e^{-1.84E}). \qquad (8)$$

The muon neutrinos from kaon decay have a harder spectrum than the pion-decay component so that it gives a significant contribution to the neutrino spectrum at about 2 GeV. The kaon-decay neutrino spectrum as a function of ν_μ energy can be approximated by the expression

$$I_{(K)}(E) \simeq \frac{n_\chi^2 \langle\sigma v\rangle_A c\tau}{4\pi} (0.73e^{-0.76E}) \qquad (9)$$

The energies of all light leptons produced in each of the other processes respectively are similar. Neutrino spectra of ν_e's ($\bar{\nu}_e$'s) and ν_μ's ($\bar{\nu}_\mu$'s) may be calculated from the expression

$$I(E_\nu) = Q(E_\nu)\langle\ell\rangle/4\pi \qquad (10)$$

with $\langle\ell\rangle$ being the mean-path-length of the annihilation region (e.g. through the

galactic halo). The integral spectra for M_χ = 15 GeV are shown in Fig. 4 for a galactic center source. These spectra are normalized to the upper limit on the γ-ray flux from the galactic center[26] assuming that γ-rays at this level and neutrinos could be from $\chi\chi$ annihilation.

The differential ν_e production spectrum has been calculated for 15 GeV higgsinos (or Majorana neutrinos) using a Lund model Monte Carlo program with the results given in Fig. 5.[27] These results give a spectral shape which agrees well with the spectrum obtained from the analytic calculations given in Fig. 4.

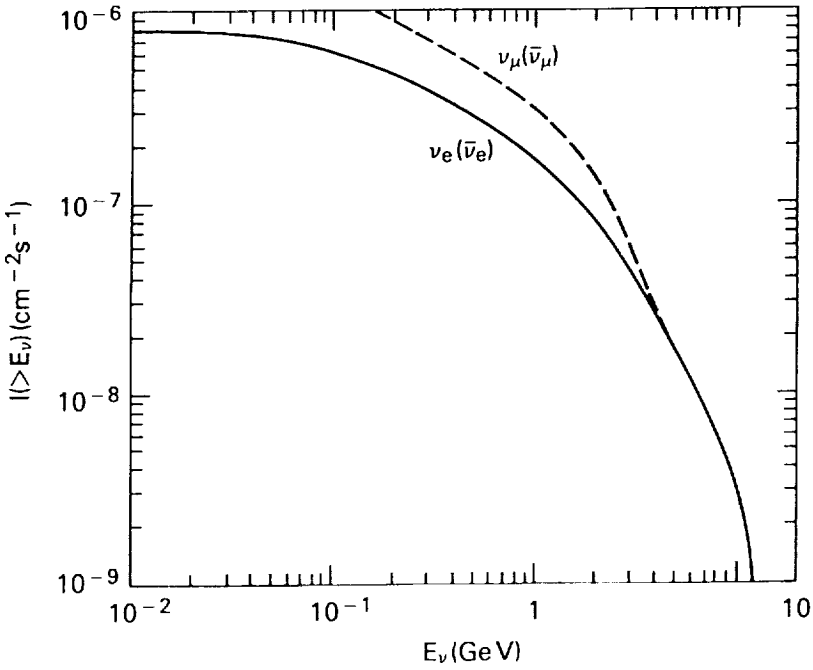

Fig. 4. The integral neutrino spectra from the galactic center normalized to the γ-ray upper limit as discussed in the text.

ANNIHILATION POSITRONS

The positron source spectrum is similar to that for neutrinos. However, the cosmic-ray positron spectrum is changed in propagating to Earth (RS) because of of energy degredation of the positrons by Compton scattering and synchrotron radiation. A detailed discussion of this is given by Rudaz and Stecker (RS). The upper limits on the low energy $\bar{p}$'s imply that positrons from $\chi\chi$ annihilation will have a flux which is expected to be significantly below that produced by cosmic ray interactions (ST1). This spectrum has been calculated using the Lund program by Tylka[13] and is shown in Fig. 6. This result is generally in good agreement with the spectral shape calculated semi-analytically by RS. However, the magnitude of the flux has been normalized taking account of the upper limits on low energy $\bar{p}$'s so that it is considerably smaller than that of RS, as well as the cosmic-ray induced flux.

THE FLUX AND SPECTRUM OF NEUTRINOS FROM SOLAR CAPTURE AND ANNIHILATION

Galactic χ particles can be captured by the gravitational field of the Sun[28] and come together in the solar interior to annihilate, with the resulting flux of solar neutrinos potentially obervable by neutrino detectors on the Earth.[29] The spectrum of solar annihilation neutrinos, which has been discussed by many authors[30]

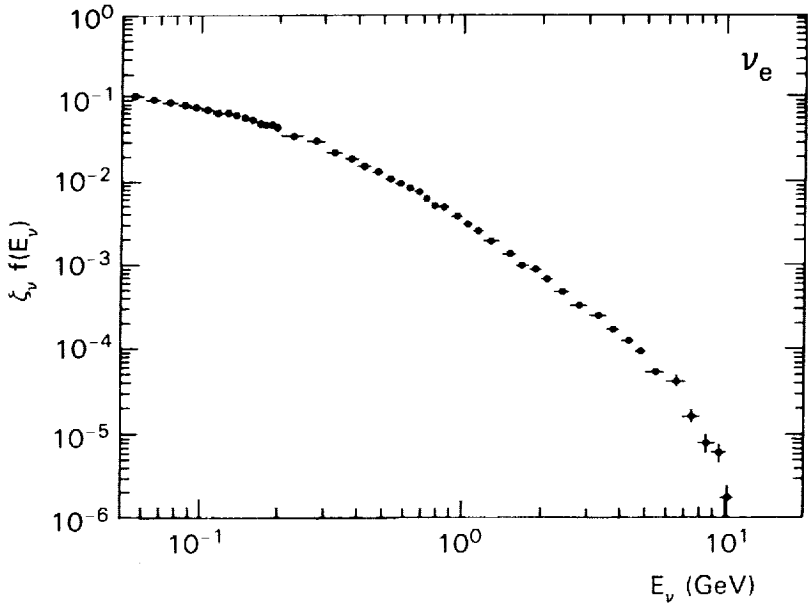

Fig. 5. The differential electron neutrino production spectrum from 15 GeV dark matter annihilation using the Lund Monte Carlo model[27]

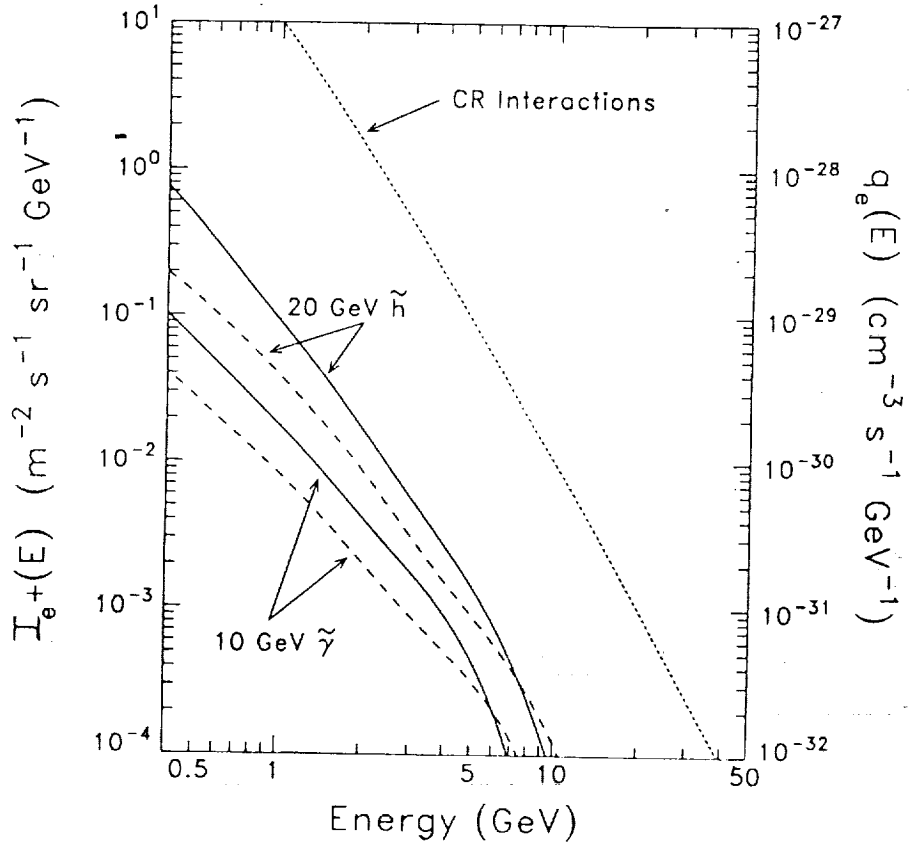

Fig. 6. The cosmic ray positron spectrum from $\chi\chi$ annihilation compared with that produced by cosmic ray interactions[13]. Source spectrum - dashed line and right hand scale; spectrum with propagation over a mean lifetime of 3×10^7 y - solid line and left hand scale.

will be significantly different from the one shown in Fig. 4, owing to the fact that muons and π's stop or interact in the solar interior before they decay. The resulting loss of ν flux or energy eliminates the π and K meson decay components and most of the second generation components from the observable spectrum. Calculations with the Lund model give a softer spectrum than most of those found previously, lowering the expected solar neutrino event rate by a factor of ~3.[9,27]

Galactic χ particles are captured and trapped by the Sun at a rate

$$\Gamma_{tr} = (3\pi/2)^{1/2}(2GM_{\odot}R_{\odot})\,\frac{n}{v}\chi\, f_{sc} \qquad (11)$$

where f_{sc} is the probability that a χ particle loses enough energy by elastic scattering to be captured[28,31]. Although lower mass χ particles can evaporate from the Sun before annihilating, those of mass > 5 GeV, with which we are concerned, will not evaporate. Then, in equilibrium, the annihilation rate will be equal to half of the trapping rate and the neutrino flux at Earth will be given by

$$I(E_{\nu}) = (\Gamma_{tr}/2)(4\pi d^2)^{-1}\zeta_{\nu}f(E_{\nu}) \qquad (12)$$

where d = 1 A.U. = 1.5 x 10^{13}cm.

For typical dark matter halo parameters $n_{\chi} = 0.4/M_{\chi}(\mathrm{GeV})$ and v = 300 km s^{-1}, the trapping rate is

$$\Gamma_{tr} \sim 10^{65}[M_{\chi}(\mathrm{GeV})]^{-1}\sigma_{p\chi\to p\chi}(\mathrm{cm}^2) \quad s^{-1}. \qquad (13)$$

For higgsinos and Majorana neutrinos, the elastic scattering cross section in eq. (13), is $\sigma \simeq 1.5 \times 10^{-38}\mathrm{cm}^2$. Taking M_{χ} = 15 GeV, we find $\Gamma_{tr} \simeq 10^{26}$ s^{-1} and the neutrino flux from solar $\chi\chi$ annihilation will be

$$I^{(\chi)}(E_{\nu}) \simeq 2 \times 10^{-2}\zeta_{\nu}f(E_{\nu}). \qquad (14)$$

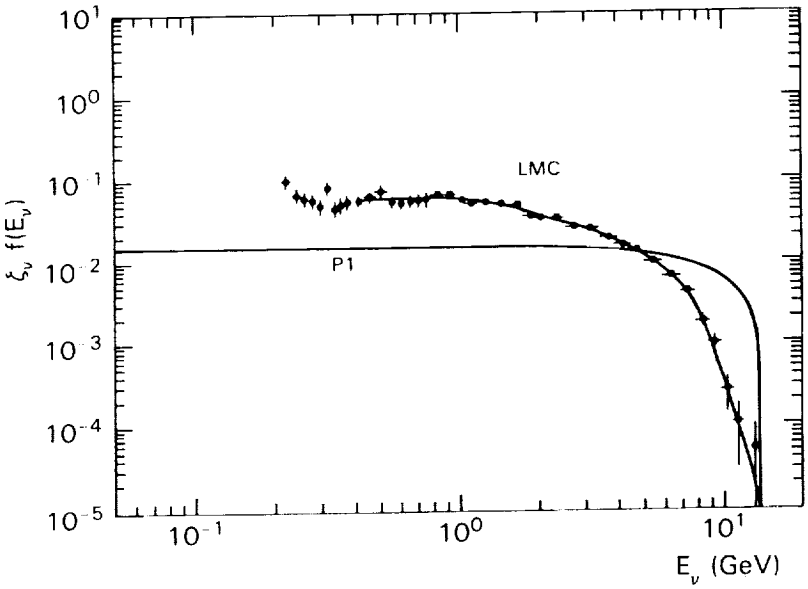

Fig. 7. The differential electron neutrino production function from 15 GeV $\chi\chi$ annihilation in the solar interior. The curve marked LMC is from the Lund Monte Carlo calculations.[27]

The total neutrino production function $\zeta_\nu f(E_\nu)$ relevant to eq. (14) is shown in Fig. 7. Fig. 7 shows both the first generation prompt (P1) approximation, similar to used in Refs. 32 and 33 and that obtained using the Lund Monte Carlo program[27], which gives a softer spectrum. Given the fluxes calculated using eq. (14), the event rate observed in a neutrino detector will be given by

$$\Gamma_{ev} = n_N \int dE\ V_{eff}(E)\ [\sigma_\nu(E_\nu) I_\nu(E_\nu) + \sigma_{\bar{\nu}}(E_{\bar{\nu}}) I(E_{\bar{\nu}})]\ , \qquad (15)$$

where V_{eff} is the effective detection volume, equal to the detector volume itself for the contained events from lower energy neutrinos (typically 0.5 to 2 GeV) and is proportional to E_ν for through going detector events of higher energy[34]. The neutrino-nucleon cross sections σ_ν and $\sigma_{\bar{\nu}}$ are linearly dependent on energy. Using eqs. (14) and (15), we can estimate the ratio of solar annihilation to atmospheric events for the IMB neutrino detector, following the discussion of Ng, et al.[30]. For contained events, this ratio is just

$$R_C = (4\pi/\Omega_\Theta)_C\ [\int_{0.5}^{2} dE\ E\ I_\nu^{(x)}(E)] \ /\ [\int_{0.5}^{2} dE\ E\ I_\nu^{ATM}(E) = 0.03 \qquad (16)$$

where Ω_Θ is the solid angle around the Sun, determined by the detector resolution, while for through going events it is

$$R_T = (4\pi/\Omega_\Theta)_T\ [\int_{2}^{M_X} dE\ E^2\ I_\nu^{(x)}(E)] \ /\ [\int_{2}^{\infty} dE\ E^2\ I_\nu^{ATM}(E)] = 1.5 \qquad (17)$$

using the production function from the Lund model. Fig. 8 shows this production function along with the P1 approximation and a typical E^{-3} atmospheric spectrum (all

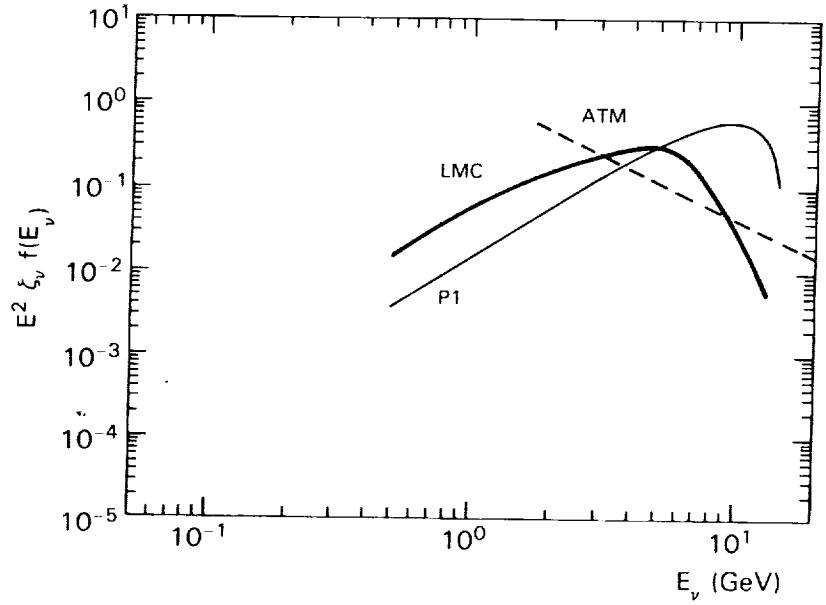

Fig. 8. Relative event rate predictions as a function of energy for solar dark matter annihilation and typical atmospheric neutrino fluxes[27]. Curve P1 and LMC are as in Fig. 6. The atmospheric spectrum is typically an E^{-3} power law[35].

weighted by E^2 as relevant to the throughgoing event rate,). This figure illustrates (1) that the event rate is overestimated by a factor of ~3 by the simple first generation approximation, and (2) that the best "window" for observing solar annihilation neutrinos is the 2-10 GeV energy range.

ANNIHILATION GAMMA RADIATION

The spectrum of γ-ray background radiation from $\chi\chi$ annihilation in the halo may be calculated by noting that the continuum flux is overwhelmingly due to the decay of neutral pions produced in the $\chi\chi$ annihilations. One can then make use of the pion production spectrum (7) in order to determine the γ-ray spectrum.[36]

The γ-ray spectrum resulting from the decay of the neutral pions is given by[37]

$$\zeta_\gamma f(E_\gamma) = 2\int_{E_\ell(E_\gamma)}^{M_\chi} dE_\pi \, (E_\pi^2 - m_\pi^2)^{-1/2} \zeta_\pi f(E_\pi) \qquad (18)$$

where $E_\ell(E_\gamma) = E_\gamma + m_\pi^2/4E_\gamma$ and ζ_γ is the γ-ray multiplicity.

A more exact calculation can be made again using the Lund Monte Carlo program[12] (ST2). For χ particles below the b quark threshhold ($M_\chi \simeq 5$ GeV), ~90% of the resulting γ-rays are from π^0 decay. The remaining 10% come from the decay of other hadrons. For larger mass χ particles, a component from B* meson decay produces a distinctively hard spectral signature in the ~0.1 GeV energy range. This channel is

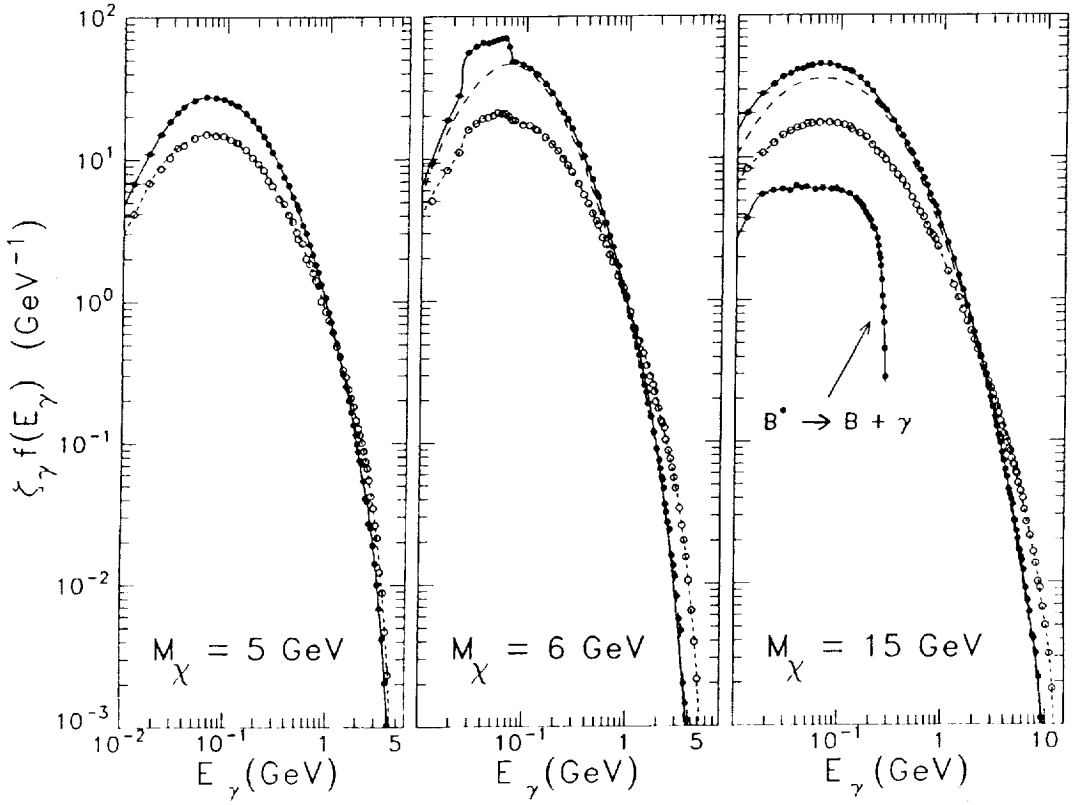

Fig. 9. Gamma-ray spectral production functions for photino (open circles) and higgsino (closed circes) annihilation. The dashed longer curves show the pion decay component only. The 15 GeV plot shows the B* decay component from $b\bar{b}$ annihilation separately.

especially important for $\tilde{h}$'s which annihilate into a $b\bar{b}$ pair ~85% of the time. In this case, γ-ray production occurs ~85% through pion decay, ~8% through B* decay and ~7% through other channels. Since $\tilde{\gamma}$'s have much smaller branching ratios for b production (~15%), B* decay accounts for only about 2% of the γ-ray production in their annihilations. Fig. 9 shows the results obtained by Stecker and Tylka[12] (ST2) for $\tilde{\gamma}$'s (closed circles) and $\tilde{h}$'s (or ν_M's)(open circles) with masses of 5, 6 and 15 GeV expressed as the quantity $\zeta_\gamma f(E_\gamma)$, where ζ_γ is the average γ-ray multiplicity per annihilation and $f(E_\gamma)$ is the normalized spectral distribution function. The π^0-decay component, is shown by a dashed line. The most striking feature is the contribution from $B^* \rightarrow B + \gamma$ decay, particulary for $\tilde{h}\tilde{h}$ annihilation. The decays $B^* \rightarrow B + \gamma$ produce a γ-ray line of energy $E^* = 51.7$ MeV in the B* rest frame. For isotropic decays, this line transforms to a square wave spectrum in the c.m. frame of the $\chi\chi$ annihilation with sharp drops at the cutoff energies[37]. For $M_\chi = 15$ GeV, the cutoff energies are 281.4 MeV and 9.5 MeV (see Fig 9).

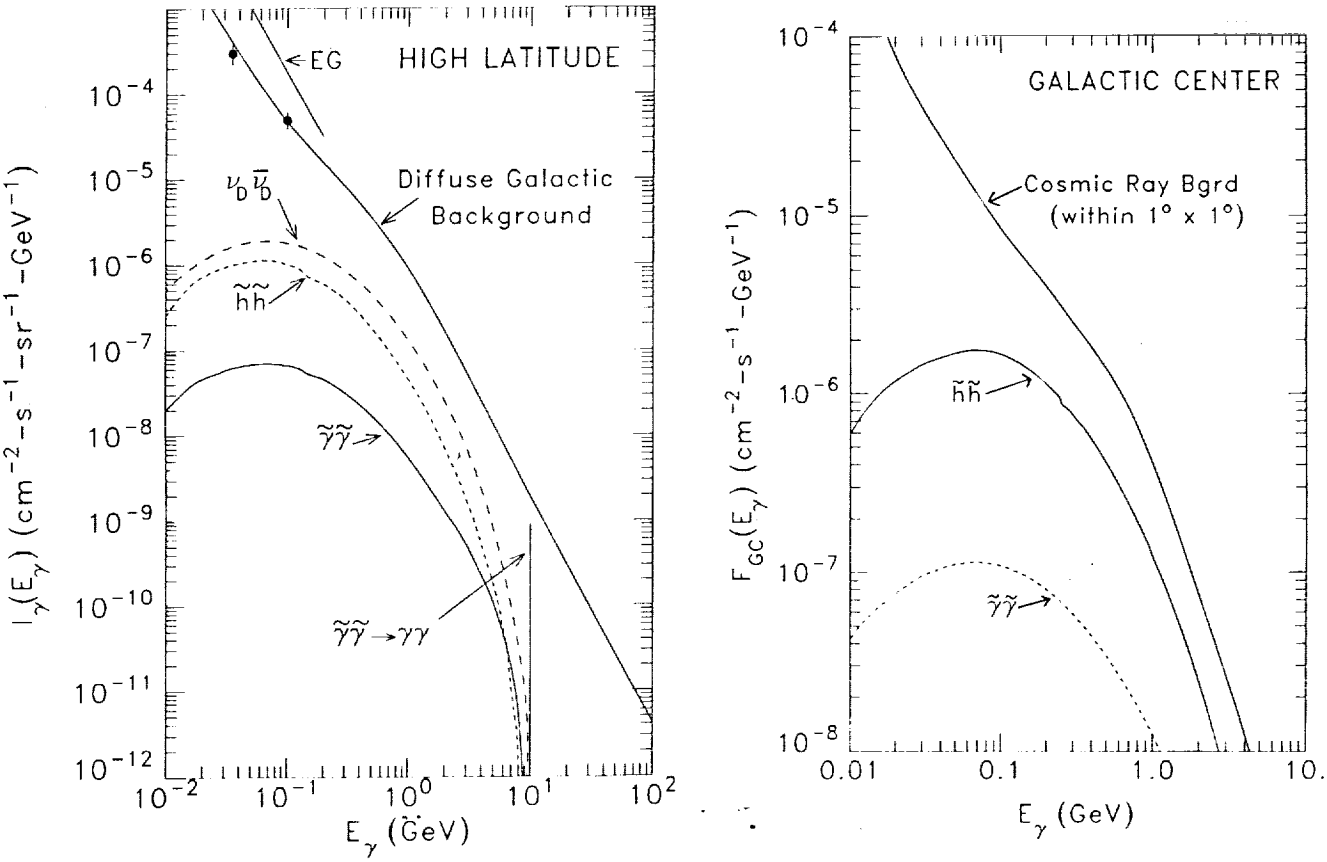

Fig. 10. The high latitude galactic γ-ray spectrum calculated for various 10 GeV χ particle annihilations compared with the extragalactic (EG) diffuse background and galactic disk radiation (see text).

Fig. 11. The annihilation spectrum from a hypothetical dark matter core at the galactic center consisting of either 15 GeV $\tilde{\gamma}$'s or $\tilde{h}$'s compared with the γ-ray flux at the galactic center from cosmic ray interactions.

The high latitude galactic γ-ray spectrum from $\chi\chi$ annihilation is (RS)

$$I(E_\gamma) = \frac{\langle \ell \rangle}{4\pi} n_\chi^2 \langle \sigma v \rangle_{ann} \zeta_\gamma f(E_\gamma)$$
$$\simeq 1.8 \times 10^{-6} \langle \ell_8 \rangle \rho_{0.3}^2 M_\chi^{-2} \langle \sigma v \rangle_{26} \zeta_\gamma f(E_\gamma) \quad cm^{-2} s^{-1} sr^{-1} \qquad (19)$$

where $\langle \ell \rangle$ is the mean line-of-sight through the galactic halo in units of 8 kpc, $\rho_{0.3}$ is the χ density in units of 0.3 GeV cm^{-3}, and the annihilation cross section is in units of 10^{-26} $cm^3 s^{-1}$. The fluxes at high galactic latitudes from the annihilation of 10 GeV $\tilde{h}$'s and 10 GeV $\tilde{\gamma}$'s are shown in Fig. 9 for $\rho_{0.3} = 1$ and $\langle \ell_8 \rangle = 1$. The generic $\tilde{h}$ cross section is $\langle \sigma v \rangle_{26} = 1.26$. For $\tilde{\gamma}$'s, ST[2] took a cross section corresponding to a lower limit on the squark mass of $\sim M_W \simeq 80$ GeV, which gives $\langle \sigma v \rangle_{26} = 0.22$.

The annihilation fluxes are compared in Fig. 10 with an estimate of the mean diffuse background flux expected from cosmic-ray interactions with interstellar gas in the galactic disk at high galactic latitudes (mean total column density of $\sim 4 \times 10^{20}$ cm^{-2})[12,38]. However, the high latitude interstellar medium is very patchy. Recent high resolution 21cm measurements, have shown that there are regions covering ~1% of the sky with neutral column densities $\leq 0.9 \times 10^{20}$ cm^{-2} (Ref. 39). In these regions, it may be possible to observe annihilation γ-radiation from a "naked" dark matter halo using a high angular resolution γ-ray telescope.[12,40]

There appears to be an extragalactic background of γ-radiation (curve EG in Fig. 10) which is softer than the galactic high latitude background[41,42]. The extragalactic flux may exceed the high latitude galactic background for energies below 0.4 GeV and may be comparable to the galactic component at higher energies provided that one can extrapolate from the observations. However, some theoretical models indicate that the extragalactic spectrum may steepen significantly above the observed energy range[43].

In addition to a γ-ray continuum, dark matter annihilation can produce line radiation in the GeV γ-ray region. For photinos of mass greater than 4 GeV and taking a minimal squark mass, Rudaz[44] finds that the line flux in the direction of the galactic pole will be

$$F_{\tilde{\gamma}\tilde{\gamma} \to \gamma\gamma} \simeq 1 \times 10^{-11} \rho_{0.3}^2 \langle \ell_8 \rangle \quad (cm^2 s \cdot sr)^{-1} \qquad (20)$$

independent of mass, with the line centered around M_χ and having a Doppler width given by $\Delta E_\gamma / E_\gamma = \beta_\chi \simeq 10^{-3}$. It follows that if an energy resolution of 10^{-3} could be obtained, the line-to-continuum ratio in a bin centered around the line would be

$$F_{line}/F_g \simeq 0.7 \, (E_\gamma / 10 \text{ GeV})^{1.7}. \qquad (21)$$

Even with a 1% energy resolution, such lines should be detectable.

It is possible for dark matter χ particles to be concentrated in a core at the galactic center by the drag of ordinary baryonic matter through collapse in the early stages of galaxy formation[45]. Annihilations from such a source at a distance r_s consisting of χ's in a volume V_s with mean-square density $\langle \rho_\chi^2 \rangle$ will give a flux

$$F(E_\gamma) = (4\pi r_s^2)^{-1} \langle \rho_\chi^2 \rangle M_\chi^{-2} \langle \sigma v \rangle V_s \zeta_\gamma f(E_\gamma) \quad (cm^2 s)^{-1}. \qquad (22)$$

Using the isothermal core model of Ipser and Sikivie[46], we find

$$(4\pi r_s^2)^{-1} V_s \langle \rho_\chi^2 \rangle \simeq 6.9 \times 10^{20} \quad GeV^2 cm^{-5}. \qquad (23)$$

For such a core of 15 GeV $\tilde{h}$'s, the γ-ray flux is given by

$$F_{GC}(0.15) \simeq 1.5 \times 10^{-6} \quad (cm^2 s \cdot GeV)^{-1} \qquad (24)$$

with a relatively flat spectrum between 0.1 and 0.2 GeV owing to B^* decay. This spectrum is much harder than the γ-ray spectrum from cosmic-ray interactions in the Galaxy, which acts as a foreground source. Both cosmic-ray (CR) induced and 15 GeV χ annihilation spectra are shown in Fig. 11 for a γ-ray telescope with a 1^o beam size. The (CR) spectrum for the inner galaxy has been calculated theoretically for the inner galaxy and agrees well with the observational data[47]. Let us consider the observablity of such a source with the EGRET γ-ray telescope to be launched on the Gamma Ray Observatory (GRO). This telescope has (1) an angular resolution of the order of 1^o in the 0.1-0.2 GeV energy range, (2) an effective area of ~1500 cm^2 in this energy range, and (3) an energy resolution of ~15%[48]. Dividing up its 80-200 MeV data into 3 energy bins of ~40 MeV each, with a 1 month exposure time, even the lowest energy bin would produce a signal of ~7σ. Using an on-off subtraction technique would further define the galactic center source. A detailed discussion of this work may be found ST2.

The extragalactic and cosmological γ-ray background spectrum from neutral heavy fermion annihilation can be calculated following the methods given by the author[49]. and can be shown to be negligible compared to the observed extragalactic background.

CONCLUSIONS

We have discussed the annihilation physics of exotic dark matter particles, in particular, those predicted by supersymmetry theory. This physics leads to the production of calculable, and potentially observable fluxes of cosmic-ray and cosmic γ-ray annihilation products. We conclude that a study of cosmic-ray antiprotons may give information about the nature of the dark matter, assuming that it is made up of χ particles. In addition, studies of galactic γ-radiation may also shed light on the dark matter problem. A characteristically hard spectrum in the 100 MeV region from a source at the galactic center or at high galactic latitudes could serve as a signature of χ particle annihilation. With significantly more sensitive γ-ray telescopes, the discovery of monochromatic radiation in the several GeV range would provide the most conclusive evidence. Solar neutrinos of several GeV energy may also give an observable signature for galactic χ particle dark matter. However, the positron flux from dark matter annihilation would be buried below that from cosmic-ray produced secondaries.

Acknowledgment: The author would like to thank Dr. A. J. Tylka for helpful discussions regarding the manuscript and for providing Fig. 6.

REFERENCES

1. Zwicky, F., 1933, Helv. Phys. Acta **6**, 110.
2. Rubin, V., et al., 1985, Astrophys. J. **289**, 81.
3. Hegyi, D. J and K. A. Olive, 1983, Phys. Lett. **126B** 28.
4. Trimble, V., 1987, Ann. Rev. Astron. Astrophys. **25**, 425.
5. Primack, J. R., et al., 1988, Ann. Rev. Nucl. Part. Sci. **38**, 751.
6. Ellis, J., et al., 1984, Nucl. Phys. **B238**, 453.
7. Greist, K., 1988, Phys. Rev. **D38**, 2357.
8. Sjöstrand, T., 1986, Comp. Phys. Comm., **39**, 347.
9. Ritz, S. and Seckel, D., 1988, Nucl. Phys. **B304**, 877.
10. Ellis, J., et al., 1988, Phys. Lett. **B214**, 403.
11. Stecker, F. W. and Tylka, A. J., 1989 Astrophys. J. Lett. **336**, L51 (ST1).
12. Stecker, F. W. and Tylka, A. J., 1989, Astrophys. J. **343**, 169 (ST2).
13. Tylka, A. J., 1989, Phys. Rev. Lett. **63**, 840.

14. Ahlen, S. P., et al., 1987, Phys. Lett. **B195**, 603.
15. Rudaz, S. and F. W. Stecker, 1988, Astrophys. J., **325**, 16.
16. Stecker, F. W., Rudaz, S. and Walsh, T. F., 1985, Phys. Rev. Letters **55**, 2622.
17. Streitmatter, R. E., et al., 1988, Adv. Space Sci., in press.
18. Ahlen, S. P. et al., 1988, Phys. Rev. Letters **61**, 145.
19. Bogomolov, E. A., et al., 1987, Proc. 20th Intl. Cos. Ray Conf. (Moscow) **2**, 72.
20. Golden, R. L., et al., 1984, Astrophys. Lett. **24**, 75.
21. Ginzburg, V. L. and V. S. Ptuskin, 1976, Rev. Mod. Phys. **48**, 161.
22. Garcia-Munoz, M., Mason, G. M., and Simpson, J. A., 1977, Ap. J. **217**, 859.
23. Webber, W. R., 1983, in Composition and Origin of Cosmic Rays, ed. M. M. Shapiro (Dordrecht: Reidel) p.25.
24. Müller, D., 1988, Adv. Space Sci., in press.
25. Flores, R. A., 1988, Phys. Lett. **B215**, 73.
26. Blitz, L., et al., 1985, Astron. Astrophys. **143**, 267.
27. Stecker, F. W. and Tylka, A. J., 1989, in preparation.
28. Press W. H., and Spergel, D. H., 1985, Astrophys. J. **296**, 679.
29. Srednicki, M., Olive, K. A., and Silk, J., 1987, Nucl. Phys. **B279**, 804.
30. Ng, K.-W., et al., 1987, Phys. Lett B **188**, 138 and refs. therein.
31. Krauss, L. M., et al., 1986, Phys. Rev. **D33**, 2079.
32. Gaisser, T. K., et al., 1986, Phys. Rev. **D34**, 2206.
33. Hagelin, J. S., et al., 1986, Phys. Lett. **B180**, 375.
34. Gaisser, T. K. and Stanev, T., 1984, Phys. Rev. **D30**, 985.
35. Perkins, D. H., 1984, Ann. Rev. Nucl. Particle Sci. **34**, 1.
36. Stecker, F. W., 1988, Phys. Lett B, **201**, 529.
37. Stecker, F. W., 1971, Cosmic Gamma Rays, Mono Book Co., Baltimore.
38. Stecker, F. W., 1989, Proc. GRO Workshop, in press.
39. Elvis, M., Lockman, F. J. and Wilkes, B. J. 1989, Astron. J., **97**, 777.
40. Silk, J., 1989, Nucl. Phys. B, in press.
41. Fichtel, C. E., et al., 1977, Astrophys. J. **217**, L9.
42. Thompson, D. J. and Fichtel, C. E., 1982, Astron. Ap., **109**, 352.
43. Stecker, F. W., 1989, Nucl. Phys. B, in press.
44. Rudaz, S., 1989, Phys. Rev. **D39**, 3549.
45. Zel'dovich, Ya. B., et al., 1980, Sov. J. Nucl. Phys. **31**, 664.
46. Ipser, J. R. and Sikivie, P., 1987, Phys. Rev. **D35**, 3695.
47. Stecker, F. W., 1989, in Cosmic Gamma Rays, Neutrinos and Related Astrophysics, ed. M. M. Shapiro and J. P. Wefel, (Dordrecht: Kluwer Academic Pub.), p. 85.
48. Thompson, D. J., 1986, Nucl. Instr. Methods, **A251**, 390.
49. Stecker, F. W., 1978, Astrophys. J. **223**, 1032.